

Implementation of a Dipole Constant Directivity Circular-Arc Array

Kurtis Manke and Richard Taylor
May 31, 2017

Thompson Rivers University, Kamloops BC, Canada

Correspondence should be addressed to Kurtis Manke (mankek12@mytru.ca)

ABSTRACT

We briefly present the theory for a broadband constant-beamwidth transducer (CBT) formed by a conformal circular-arc array of dipole elements previously developed in seminal works. This technical report considers a dipole CBT prototype with cosine amplitude shading of the source distribution. We show that this leads to a readily-equalizable response from about 100Hz to 10kHz with a far-field radiation pattern that remains constant above the cutoff frequency determined by the beam-width and arc radius of the array, and below the critical frequency determined by discrete element spacing at which spatial aliasing effects occur. Furthermore, we show that the shape of the radiation pattern is the same as the shading function, and remains constant over a broad band of frequencies.

1 Introduction

Taylor, Manke and Keele in [1] developed the theory for a constant directivity circular-arc (CBT) line arrays formed by continuous line sources of dipole elements. They have shown that choosing an appropriate frequency-independent amplitude shading function leads to a far-field radiation pattern that is constant above a cutoff frequency determined by the beam-width and arc radius of the array.

In this report we examine the results of a prototype CBT dipole array, and show that it confirms much of the existing theory.

2 CBT Theory Review

The following are key results from [1] with most of the steps omitted. See the original paper for more details.

We consider a time-harmonic acoustic line source in the form of a circle of radius a , in free space, as shown in Fig. 1. The source elements are taken to be radially-oriented dipoles. We adopt a coordinate system in which the circle lies in the xz -plane, with its center at the origin. We take the x -axis ($\theta = \phi = 0$) to be the primary “on-axis” direction of the resulting radiation pattern. We assume the source distribution is iso-phase and continuous, with strength that varies with polar angle α according to a dimensionless and frequency-independent “shading function” $S(\alpha)$ (sometimes also called the amplitude taper).

We assume the shading function $S(\alpha)$ is even, so it can be expressed as a Fourier cosine series

$$S(\alpha) = \sum_{n=0}^{\infty} a_n \cos(n\alpha) \quad (1)$$

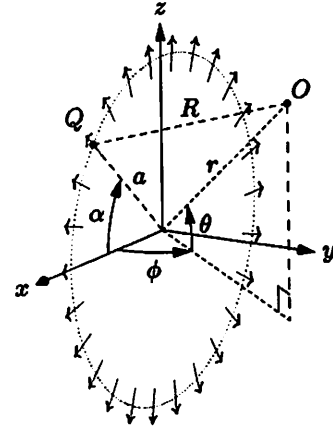


Fig. 1: Geometry of a circular line source of dipoles.

Referring to Fig. 1, the total (complex) pressure at O in the far-field due to a line source of dipole elements, with unit acceleration amplitude, is given by

$$p = \frac{e^{-ikr}}{r} ka \cos \phi \sum_{n=0}^{\infty} a_n f_n(ka \cos \phi) \cos(n\theta) \quad (2)$$

where k is the wave number [2, p. 312] and with

$$f_n(x) = 2\pi i^n J'_n(x) \quad (3)$$

where J_n is a Bessel function of the first kind [3].

Taylor, et al. go on to derive the following properties from (2):

- Each circular harmonic shading mode is mapped to a corresponding radiation mode in the far field

by a factor f_n (the “mode amplitude”) that depends only on ϕ and the dimensionless frequency ka , thus preserving the mode shape. Hence, any single-mode shading $S(\alpha) = \cos(n\alpha)$ the far-field radiation pattern is identical to the shading function at all frequencies, at least in any vertical plane (constant ϕ).

- The far-field radiation pattern of an appropriately shaded circular array of dipoles will be independent of frequency provided

$$x = k a \cos \phi \gg n \quad (4)$$

- For frequencies above cutoff the far-field pressure decreases at 3 dB/oct with decreasing frequency.
- Below cutoff, the array as a whole radiates like a single dipole at the origin, oriented along the x -axis. Hence, the far-field pressure decreases at 6 dB/oct with decreasing frequency.

3 Experimental Prototype

A single dipole CBT array was constructed using 10 full-range audio transducers with no cabinet. It was designed to have -6dB beamwidth at 47° , where the array formed a 70° circular arc, with a radius of 705 mm, and a source spacing of 66 mm (centre-to-centre).

The prototype used 10 ND65-8 2.5” full-range drivers produced by Dayton Audio. These drivers feature a usable frequency range from 80 Hz to 20 kHz, low distortion, and 15 W of RMS power handling [4]. The array is shown in Fig. 2.

3.1 Shading Function

The shading function $S(\theta)$ implemented in our prototype

$$S(\theta) = \begin{cases} \cos\left(\frac{\theta}{7}\right) & |\theta| \leq 70^\circ \\ 0 & |\theta| > 70^\circ \end{cases} \quad (5)$$

was chosen from a list of several good candidate shading functions provided by Taylor, et al. [1]. It is important to note that the array will be mirrored by a ground-plane reflection [5], and the shading function in (5) is symmetric about $\theta = 0^\circ$. Thus an array on the ground with a circular arc from $\theta = [0^\circ, 70^\circ]$ should have the same response as an array in free-space with a circular arc from $\theta = [-70^\circ, 70^\circ]$.

Each driver in the array is shaded by sampling (5) at the driver’s angle from horizontal. A circuit diagram for the network is shown in Fig. 3. Although there are many different ways one could design a shading network, this one was chosen because it incorporates

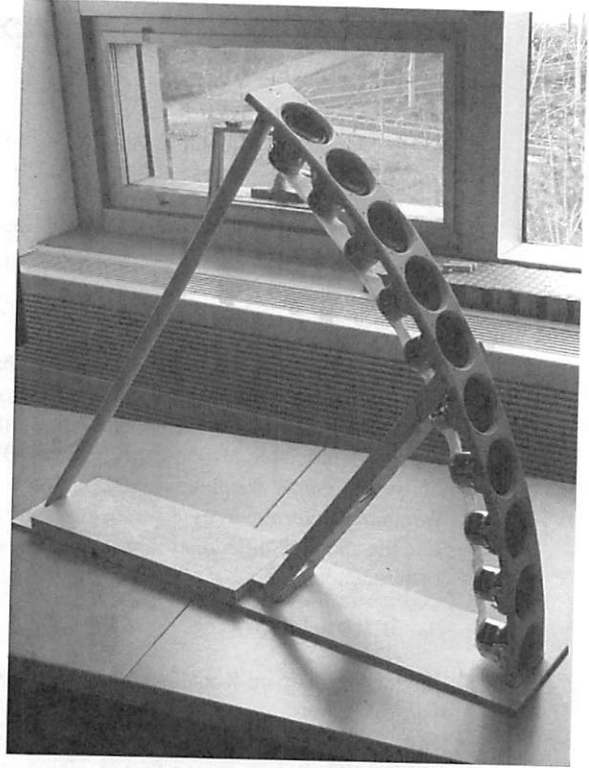


Fig. 2: The fully assembled dipole array.

resistances which are easily implemented with no more than three typical (“off-the-shelf”) resistors (in series and parallel combinations), the circuit does an adequate job of minimizing power loss through the resistors, the circuit is easy to assemble, and the total impedance of each branch is such that the total input impedance is between 4Ω and 8Ω (impedances that almost any audio amplifier can handle). The shading circuit was CNC milled onto double-sided copper clad board, and the amplifier and drivers were connected to the board using screw terminals and 18-gauge wire, shown in Fig. 4.

This method has advantages over the point-to-point wiring used in previous CBT implementations [6] as it allows potential for changing shading functions simply by switching to a different board, and it greatly simplifies the assembly process.

3.2 Magnitude Response

The array was measured at a variety of angles using a microphone placed two meters away. A maximum length sequence (MLS) signal was played through the array for a total of 3 seconds to generate an impulse response. The frequency response is extracted from the impulse response by applying a modified Hadamard transform, a common technique in acoustics [7, Ch. 6].

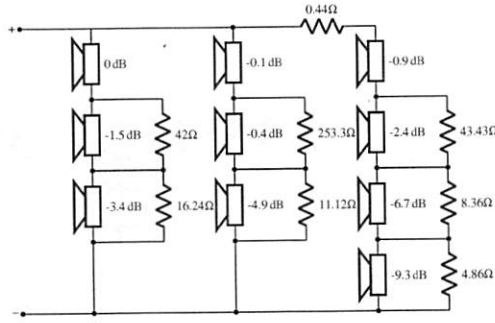


Fig. 3: Resistive network designed to implement the shading function in (5).

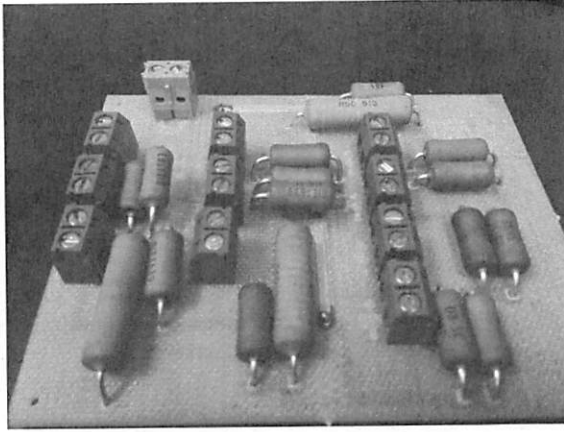


Fig. 4: the CNC milled shading circuit from Fig. 3.

Ideally, all testing would have been done in an anechoic chamber. Lacking access to one, a large, quiet, and open space should be used. Hence, all measurements were made in the Thompson Rivers University gymnasium. Fortunately, the floor reflection is part of the CBT design so the next closest reflecting surface was the roof of the gymnasium, located 8 metres away. It was assumed that the speed of sound in air was 343 m/s, thus the first reflection took around 60 ms to reach the microphone. To remove all reflections from the measurement, only the first 55 ms of the measurement are used.

The raw (unequalized) magnitude response for the on-axis response is shown in Fig. 5. It is clear that above the cutoff frequency the level drops at 3 dB/oct toward low frequency as predicted by the theory. Below cutoff it was predicted that the level would drop 6 dB/oct toward low frequency, however, this was not observed. In this report, we only offer some speculations as to why the array did not behave as expected below cutoff:

- The impedance of the drivers increases rapidly

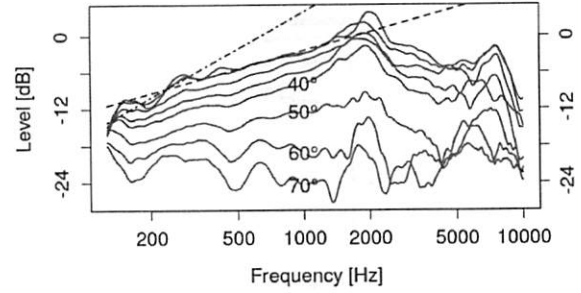


Fig. 5: The (unequalized) magnitude response of the dipole CBT array from $\theta = [0^\circ, 70^\circ]$ (blue), and 3 dB/oct (dashed) and 6 dB/oct (dash-dot) at the cutoff frequency.

below 300 Hz [4], so the shading circuit becomes less effective at attenuating the low-level drivers.

- Although the gymnasium was relatively quiet, the HVAC system could not be disabled during testing, which may have introduced significant noise at frequencies below 100 Hz.

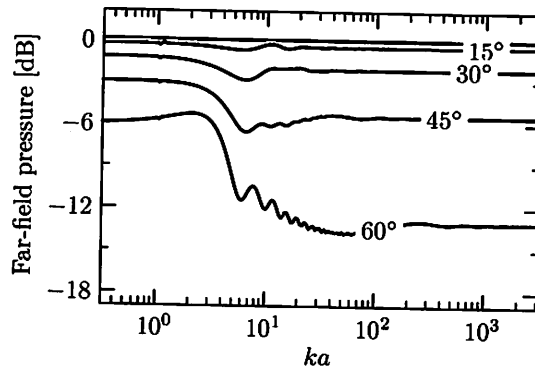
In any case, we are left with a system that can be readily equalized between 100 Hz and 10 kHz. Fig. 6 shows both the (normalized) simulated response and the measured response. It is clear that there is considerably more ripple in the measured response, but the spacing between θ responses remains fairly constant, which indicates that radiation pattern maintains roughly the same shape.

The radiation pattern at several different frequencies, along with the shading function, are shown in Fig. ???. Note that the radiation pattern emulates the shape of the shading function closely, as predicted.

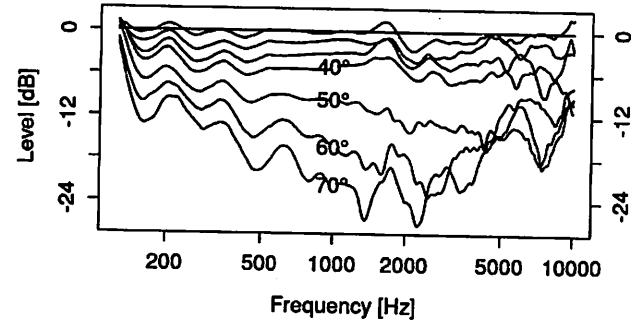
4 Conclusion

We have shown that a practical device implementing the theory developed in [1] can be formed using a discrete array of conventional drivers and confirmed many predictions from their work, including:

- The far-field radiation pattern has the same shape as the shading function for a single-mode shading function (e.g. cosine shading).
- The far-field radiation pattern remains constant above a cutoff frequency, until spatial aliasing effects occur.



(a) Simulated response.



(b) Measured response.

Fig. 6: Far-field magnitude responses at various angles θ in the plane of the array, normalized to the on-axis ($\theta = 0$) response, for a circular-arc array of dipole source elements. The shading in both cases is the wide-beam cosine shading of equation (5).

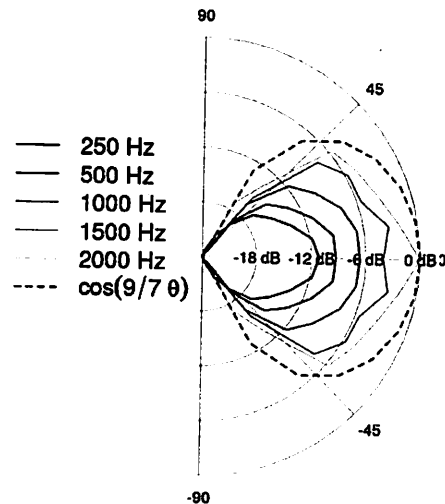


Fig. 7: The far-field radiation pattern (equalized to the maximum on-axis level) for several different frequencies (solid), as well as the shape of the shading function from (5) (dashed).

- Above cutoff, the on-axis response level drops at 3 dB/oct.

In subsequent works, we would like to address the issue of the measured response below cutoff differing from that predicted by the theory.

Acknowledgments

This research was supported through a UREAP grant provided by Thompson Rivers University. The authors would also like to gratefully acknowledge the use of the services and facilities of Thompson Rivers University.

Portions of this study will be presented at the 143rd Audio Engineering Society Convention, New York, NY, on October 18–21, 2017.

References

- [1] Taylor, R., Manke, K., and Keele, Jr., D. B., "Constant directivity circular-arc arrays of dipole elements," in *Audio Engineering Society Convention 143*, Audio Engineering Society, 2017, manuscript submitted for peer review.
- [2] Morse, P. M. and Ingard, K. U., *Theoretical Acoustics*, Princeton University Press, 1987.
- [3] DLMF, "NIST Digital Library of Mathematical Functions," <http://dlmf.nist.gov/>, Release 1.0.13, 2016, F. W. J. Olver, A. B. Olde Daalhuis, D. W. Lozier, B. I. Schneider, R. F. Boisvert, C. W. Clark, B. R. Miller and B. V. Saunders, eds.
- [4] ND65-8 2-1/2" Aluminum Cone Full-Range Driver 8 Ohm, Dayton Audio, n.d.

- [5] Keele, Jr., D. B., "Use of ground-plane constant beamwidth transducer (CBT) loudspeaker line arrays for sound reinforcement," in *Audio Engineering Society Convention 141*, Audio Engineering Society, 2016.
- [6] Keele, Jr., D. B., "Practical implementation of constant beamwidth transducer (CBT) loudspeaker circular-arc line arrays," in *Audio Engineering Society Convention 115*, Audio Engineering Society, 2003.
- [7] Havelock, D., Kuwano, S., and Vorländer, M., editors, *Handbook of Signal Processing in Acoustics*, Springer-Verlag New York, 2008.